DEMONSTRATION OF REPEAT-PASS POLINSAR USING UAVSAR: THE RMOG MODEL

Marco Lavalle and Scott Hensley

Jet Propulsion Laboratory, California Institute of Technology

ABSTRACT

In this paper we show our first POLINSAR results using the Uninhabited Aerial Vehicle Synthetic Aperture Radar (UAVSAR) developed by the Jet Propulsion Laboratory (JPL). UAVSAR is a L–band repeat-pass polarimetric and interferometric system designed for measuring vegetation structure and monitoring crustal deformations. In order to extract canopy height from POLINSAR data and account for temporal decorrelation, we formulate a physical model of the temporal-volumetric coherence, random motion over ground (RMOG) model. Canopy height extracted from single-baseline UAVSAR data using the RMOG model is shown to be in agreement with canopy height measured by the Land, Vegetation, and Ice Sensor (LVIS) lidar.

Index Terms— Synthetic aperture radar, polarimetry, interferometry.

1. INTRODUCTION

Polarimetric SAR interferometry (POLINSAR) [1] is a mature technique applied to measure Earth's vegetation properties from space. A polarimetric interferometer consists of a radar antenna that illuminates a patch of the Earth's surface from two different orbital positions to generate two single look complex (SLC) images. The complex correlation coefficient (or coherence) between two complex images obtained with arbitrary combination of transmit and receive polarization contains information about the imaged surface and is exploited to measure forest properties [2].

The coherence is typically decomposed in several decorrelation contributions: the geometric-surface decorrelation, the volumetric decorrelation, the temporal decorrelation, and the thermal-noise decorrelation [3]. In previous works, forests properties have been extracted from measures of *volumetric* coherence. While thermal-noise and geometric surface decorrelation can be removed from the measured coherence, temporal decorrelation is difficult to be estimated from the data and represents the major limitation of repeat-pass polarimetric interferometry.

In this paper we test a new approach for extracting forest properties using polarimetric SAR interferometry. Our approach is based on a physical model of the *temporal-volumetric* coherence that accounts for both temporal and volumetric decorrelation. The model is referred to as random motion over ground (RMOG) model as the scattering scenario is borrowed from the *random volume over ground* (RVOG) model. We added dynamic properties to this scattering scenario in the form of random motion of the scattering elements to account for temporal decorrelation. The RMOG model is particularly suitable for modeling single-baseline, repeat-pass polarimetric interferometric data with short or moderate temporal baseline, for which the assumption of random motion is expected to be valid. When available, single-pass interferometric data should be preferred to repeat-pass data as temporal changes inevitably introduce phase noise and affect parameter estimation.

The paper is organized in two parts. In the first part we deal with the forward problem and summarize the properties of the RMOG model. In the second part we describe a possible inversion scheme for the RMOG model and show results of canopy height estimated from UAVSAR data. The results are presented in contrast with the canopy height estimated using the RVOG model and the canopy height measured by the LVIS lidar.

2. RANDOM MOTION OVER GROUND MODEL

In this section we discuss some important features of the RMOG model. An exhaustive derivation of the model including the improvements made over time can be found in [4, 5, 6, 7, 8, 9]. The RMOG model is a physical model of the coherence measured by a repeat-pass polarimetric interferometer over forests. The model establishes an analytical link between a small set of forest properties and the temporal-volumetric coherence.

In the model, the vegetated surface is idealized as a vertical distribution of randomly oriented scattering elements, i.e. a volume layer, with an underlying dielectric rough surface. The surface is located at $z = z_g$ and the volume layer extends between $z = z_g$ and $z = z_g + h_v$, where h_v is the thickness of the layer and z is the vertical dimension of the coordinate system. The volume layer and the underlying surface are characterized by an exponential backscatter density function per unit length. Dynamic changes are modeled as random motion of the scattering elements. The statistic of the motion is assumed to be Gaussian with zero mean and z-dependent variance $\sigma_r^2(z)$ measured along the radar line-of-sight. We

use a first-order approximation of $\sigma_r^2(z)$ to derive an explicit expression of the RMoG coherence

$$\gamma = e^{j\varphi_g}\,\frac{\mu\,\gamma_{t_g} + \gamma_{vt}\,e^{-j\varphi_g}}{\mu+1} \tag{1}$$

where

$$\gamma_{t_g} = \exp\left[-\frac{1}{2}\left(\frac{4\pi}{\lambda}\right)^2\sigma_g^2\right] \tag{2}$$

is the temporal coherence of the ground surface, and

$$\gamma_{vt} = e^{j\varphi_g}\,\gamma_{t_g}\,\frac{p_1\left[e^{(p_2+p_3)h_v}-1\right]}{(p_2+p_3)\left(e^{p_1h_v}-1\right)} \tag{3}$$

is the temporal-volumetric coherence of the volume layer without underlying surface, with

$$p_1 = \frac{2\kappa_e}{\cos(\theta-\alpha)},\;\; p_2 = p_1 + jk_z,\;\; p_3 = -\frac{\Delta\sigma^2}{2h_r}\left(\frac{4\pi}{\lambda}\right)^2. \tag{4}$$

The ground topography phase is indicated with $\varphi_g = k_z z_g$, where k_z is the vertical wavenumber of the interferometer. In (1) to (4), λ is the system wavelength, μ the effective ground-to-volume ratio, κ_e is the mean wave extinction, θ is the average look angle and α is the tilt the ground surface along range. The *differential motion variance* $\Delta\sigma^2$ and the *differential motion standard deviation* $\Delta\sigma = \sigma_v - \sigma_g$ are indicators of how much the motion is uniform along the vertical dimension. We indicated with σ_g the motion standard deviation of the scatterers located at $z = z_g$, and with σ_v the motion standard deviation of the scatterers at a reference height h_r with respect to the ground surface. The term p_3 accounts for temporal decorrelation. When $\sigma_g^2 = 0$ and $\Delta\sigma^2 = 0$ no temporal decorrelation occurs, and the RMoG model is equivalent to the RVoG model

$$\gamma_v = \frac{e^{j\varphi_g}}{\mu+1}\left[\mu + \frac{p_1\left(e^{p_2h_v}-1\right)}{p_2\left(e^{p_1h_v}-1\right)}\right]. \tag{5}$$

Similarly, when $k_z = 0$ no volumetric decorrelation occurs, and the RMoG model reduces to the temporal decorrelation model published in [6]

$$\gamma_t = \frac{1}{\mu+1}\left[\mu\gamma_{t_g} + \frac{p_1}{p_1+p_3}\,\frac{e^{(p_1+p_3)h_v}-1}{e^{p_1h_v}-1}\right]. \tag{6}$$

The RMoG model unveils a noteworthy property of the coherence measured by a repeat-pass interferometer over forests. In the presence of arbitrary motion along the vertical profile, the total coherence cannot be factorized as the product of temporal and volumetric coherence

$$\gamma \neq \gamma_v\,\gamma_t. \tag{7}$$

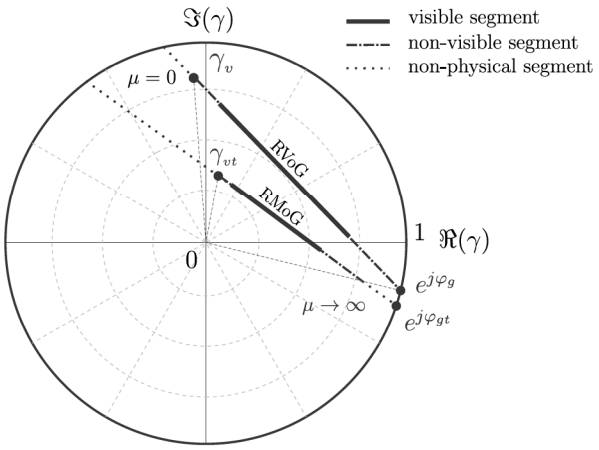

Fig. 1. Coherence loci of the RMoG and RVoG models. The RMoG line model does not intersect the unit circle at the true ground topographic phase φ_g.

It is interesting to examine the coherence locus of the RMoG model. The coherence locus is the set of coherence values obtained by varying the ground-to-volume ratio, μ. The RMoG coherence locus can be plotted in the complex plane by writing (1) in the following form

$$\gamma = \gamma_{vt} + \frac{\mu}{\mu+1}\left(\gamma_{t_g}\,e^{-j\varphi_g} - \gamma_{vt}\right), \tag{8}$$

which corresponds to the equation of a line. The RMoG coherence locus is a line segment similarly to the RVoG coherence locus. In Fig. 1 we have highlighted three regions on the RMoG coherence locus: a visible segment, corresponding to actual coherence values that are observed through polarization diversity; a non-visible segment, corresponding to coherence values that are not observed in the actual data; a non-physical segment, corresponding to invalid coherence values according to the RMoG model. The RVoG locus is also plotted for comparison. There are two key differences between the RMoG and RVoG coherence loci. First, the RMoG line does not intersect the unit circle at the true ground topography but at some point with phase $\varphi_{gt} \leq \varphi_g$. In the limit $\mu \to \infty$, the RMoG coherence phase is the true topography phase with the coherence magnitude that corresponds to the ground temporal decorrelation, which generally does not equal to one. For this reason a non-physical region appears between the points $e^{j\varphi_{gt}}$ and $\gamma_{t_g}\,e^{j\varphi_g}$.
Second, the RMoG coherence point γ_{vt} obtained for $\mu = 0$ shifts and changes magnitude and phase with respect to the RVoG volume coherence point γ_v. When $\Delta\sigma = 0$ the RMoG coherence locus is parallel to the RVoG coherence locus and γ_{vt} moves away from γ_v and towards the origin in a radial direction. When $\Delta\sigma \neq 0$ the RMoG coherence line tilts and shrinks with respect to the RVoG coherence line.

3. PARAMETER ESTIMATION USING THE RMOG MODEL

In this section we describe a possible inversion scheme for the RMOG model. Our objective is to design an algorithm to be used to extract canopy height from single-baseline, repeat-pass POLINSAR data. Consider a POLINSAR dataset of eight co-registered single-look complex images. Let assume the interferometric coherence estimated from the data to be affected mainly by temporal and volumetric decorrelation. In order to estimate the RMOG model parameters for each image sample, we start by calculating the RMOG coherence line and the intersection of the line with the unit circle as illustrated in Fig. 1. In order to do this, we estimate the coherence associated with the minimum and maximum ground-to-volume ratio, indicated in the following by $\widehat{\gamma}_1$ and $\widehat{\gamma}_5$, respectively. These two coherence points correspond to the extrema of the visible segment. They are calculated by maximizing the amplitude separation of the coherence samples obtained through polarization diversity [10]. Then we calculate the equation of the line passing through $\widehat{\gamma}_1$ and $\widehat{\gamma}_5$, and find its intersection with the unit circle [10]

$$\varphi_{gt} = \arg\left[\widehat{\gamma}_5 - \widehat{\gamma}_1\,(1 - F_5)\right] \qquad 0 \le F_5 \le 1 \tag{9}$$

where φ_{gt} is the phase of the intersection and F_5 is the solution of the quadratic equation

$$F_5 = \frac{-B - \sqrt{B^2 - 4AC}}{2A} \tag{10}$$

with $A = |\widehat{\gamma}_1|^2 - 1$, $B = 2\Re(\widehat{\gamma}_5\widehat{\gamma}_1^* - |\widehat{\gamma}_1|^2)$ and $C = |\widehat{\gamma}_5 - \widehat{\gamma}_1|^2$. The parameter F_5 represents the normalized distance between $\widehat{\gamma}_1$ and $\widehat{\gamma}_5$. This procedure of calculating the line intersection is similar to the RVOG model inversion [10] with the exception that the intersection of the RMOG line with the unit circle does not correspond to the ground topography but is shifted depending on the amount of temporal decorrelation. Although φ_{gt} does not correspond to the true ground phase, it can be used as an initial guess in the calculation of the true ground topography.

Next, we select three additional coherence points that are well separated from each other and from $\widehat{\gamma}_1$ and $\widehat{\gamma}_5$ in the complex plane. This can be done conveniently using (9)

$$\widehat{\gamma}_i = \widehat{\gamma}_1 + F_i\left(e^{j\varphi_{gt}} - \widehat{\gamma}_1\right), \quad F_i = \frac{F_5}{4}(i-1) \quad i = 1, 2, ..., 5. \tag{11}$$

The coherence points $\widehat{\gamma}_i$, $i = 1, 2, ..., 5$, represent the interferometric coherence of different scattering mechanisms with scattering phase centers located along the vertical direction in the canopy. The coherence points are associated to different values of ground-to-volume ratio μ_i, $i = 1, 2, ..., 5$, and contain different levels of temporal and volumetric decorrelation. The RMOG inverse problem may be formally stated as

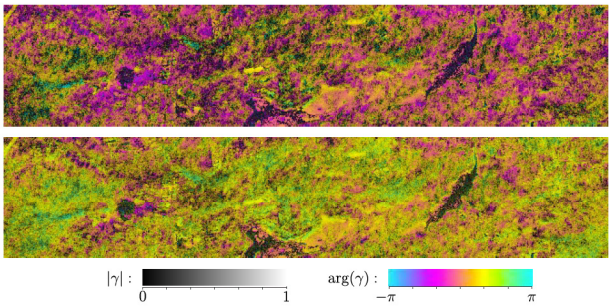

Fig. 2. Subset of UAVSAR L–band POLINSAR data collected near Harvard Forest (Massachusetts). The images show the complex coherence associated with the lowest (top) and largest (bottom) ground-to-volume ratio observed in the data.

solution of a set of 5 non-linear equations

$$\widehat{\gamma}_i\, e^{-j\varphi_{gt}} = e^{j(\varphi_g - \varphi_{gt})}\,\frac{\mu_i\,\gamma_{t_g} + \gamma_{vt}\,e^{-j\varphi_g}}{\mu_i + 1}, \quad i = 1, 2, ..., 5. \tag{12}$$

Each equation relates one coherence observation to a set of parameters according to the RMOG model. Ten unknowns (φ_g, h_v, κ_e, σ_g, σ_v, μ_1, μ_2, μ_3, μ_4, μ_5) are related to five complex coherence observations. Using (12) to invert the RMOG model has the advantage of avoiding a priori assumptions on the values of the model parameters. The solution of (12), however, might require an extensive search as it involves non-linear equations. We estimate the model parameters with a least-square optimization technique that minimizes the cost function

$$F = \sum_{i=1}^{5} \left|\gamma_i - \widehat{\gamma}_i\right|^2 \tag{13}$$

where γ_i are the RMOG model predictions. The inversion procedure described above has been successfully applied to estimate canopy height from actual UAVSAR data.

UAVSAR is the airborne radar instrument developed at Jet Propulsion Laboratory [11]. The radar instrument employs a quad-polarimetric L–band electronically scanned antenna and $8 \cdot 10^7$ Hz pulse bandwidth. In 2009 UAVSAR performed a series of flights near Harvard Forest in Massachusetts (United States). Lidar data acquired by the NASA Laser Vegetation Imaging Sensor (LVIS) in 2009 are also available.

We select a subset of the UAVSAR data where a typical forest height is between 20 m and 25 m according to lidar data. The vertical wavenumber in the subset ranges between $0.06\,\mathrm{m}^{-1}$ and $0.08\,\mathrm{m}^{-1}$. The temporal baseline is about 2 days. We estimate the coherence associated with the minimum and maximum ground-to-volume ratio, i.e., the extrema of the visible segment illustrated in Fig. 1. A subset of the two coherence images is shown in Fig. 2. Coherence is estimated by averaging data to about 100 independent looks. In the figure, the brightness of each sample is related to the coherence

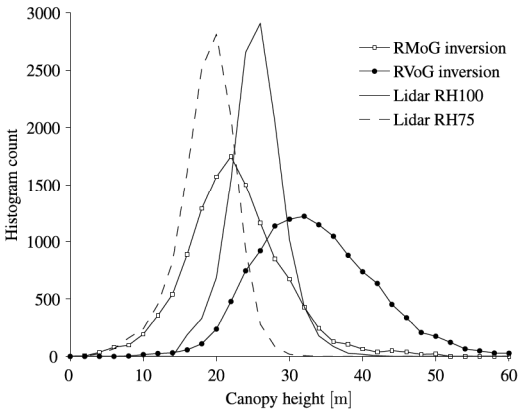

Fig. 3. Canopy height estimated from UAVSAR POLINSAR data.

magnitude while the color denotes the interferometric phase. Fig. 2 (top) shows the volume-dominated coherence $\widehat{\gamma}_1$. The average magnitude of $\widehat{\gamma}_1$ is 0.65. Fig. 2 (bottom) shows the ground-dominated coherence $\widehat{\gamma}_5$. The average magnitude of $\widehat{\gamma}_5$ is 0.57. The average phase difference height between $\widehat{\gamma}_5$ and $\widehat{\gamma}_1$ is about $8\,\mathrm{m}$.

We note that areas with high coherence and green-yellow color appear similar in the two images. These correspond to clear-cuts or low vegetated areas for which the volumetric decorrelation is small and the visible segment is short, i.e., $\widehat{\gamma}_5$ and $\widehat{\gamma}_1$ lie both very close to $e^{j\varphi_{gt}}$ in the complex plane. Areas with larger phase difference between $\widehat{\gamma}_5$ and $\widehat{\gamma}_1$ reveal the wave penetration in the canopy and the shift of the scattering phase center with polarization. Phase patterns in the figure are due to spatial variation of canopy structure, topography and temporal decorrelation.

In Fig. 3 we present the results of the RMOG canopy height in contrast with the RVOG canopy height and lidar data. Low lidar values are excluded from the analysis because they might be unreliable lidar measurements. The RVOG canopy height is overestimated due to the uncompensated temporal decorrelation. The average difference between RVOG and RMOG canopy height is larger than $10\,\mathrm{m}$. The RMOG canopy height is between the lidar canopy height RH100 and the lidar canopy height RH75. This is in agreement with the expectations as the lidar measures the height of the tallest scatterer within the footprint, whereas the radar measures the average canopy height from the multi-looked image.

The average value of σ_g is about $0.4\,\mathrm{cm}$, which gives about 0.97 temporal decorrelation at L–band. Most of the estimated values of σ_v range between $0.5\,\mathrm{cm}$ and $2\,\mathrm{cm}$. The average value of the equivalent uniform temporal decorrelation in the canopy is 0.67. In this particular dataset, we did not observe major dielectric changes within the 2-day time interval of the acquisitions. For longer time interval, however, dielectric changes are more likely to occur [12] and should be masked before applying the RMOG model inversion.

Acknowledgement

This research was conducted at Jet Propulsion Laboratory, California Institute of Technology, under contract with the National Aeronautics and Space Administration. The authors would like to thank the UAVSAR team for collecting and processing the data. Lidar data sets were provided by the LVIS team at NASA Goddard Space Flight Center.

4. REFERENCES

[1] S.R. Cloude and K.P. Papathanassiou, "Polarimetric SAR Interferometry," *Geoscience and Remote Sensing, IEEE Transactions on*, vol. 36, no. 5, pp. 1551–1565, 1998.

[2] R.N. Treuhaft, S.N. Madsen, M. Moghaddam, and van Zyl J.J., "Vegetation characteristics and underlying topography from interferometric radar," *Radio Science*, vol. 31, no. 6, pp. 1449–1485, Nov.-Dec. 1996.

[3] H.A. Zebker and J. Villasenor, "Decorrelation in interferometric radar echoes," *Geoscience and Remote Sensing, IEEE Transactions on*, vol. 30, no. 5, pp. 950–959, Sep. 1992.

[4] M. Lavalle, *Full and compact polarimetric radar interferometry for vegetation remote sensing*, Ph.D. thesis, University of Rennes 1 and University of Rome Tor Vergata, Dec. 2009.

[5] M. Lavalle, S. Hensley, and M. Simard, "Recent advances on InSAR temporal decorrelation: theory and observations using UAVSAR," in *Proceedings of Fringe Workshop 2011, European Space Agency*, Frascati, Italy, Sept. 2011.

[6] M. Lavalle, M. Simard, and S. Hensley, "A temporal decorrelation model for polarimetric SAR interferometers," *IEEE Transactions on Geoscience and Remote Sensing*, 2011 (online).

[7] M. Lavalle and M. Simard, "Temporal and volume effects in polarimetric SAR interferometry," in *Proceedings of PolInSAR workshop 2011, European Space Agency*, Frascati, Italy, Jan. 2011.

[8] M. Lavalle, M. Simard, D. Solimini, and E. Pottier, "Height-dependent temporal decorrelation in PolInSAR and TomoSAR forestry applications," in *8th European Conference on Synthetic Aperture Radar*, Aachen, Germany, Jun. 2010.

[9] M. Lavalle, M. Simard, E. Pottier, and D. Solimini, "PolInSAR forestry applications improved by modeling height-dependent temporal decorrelation," in *Geoscience and Remote Sensing Symposium (IGARSS), 2010 IEEE International*, July 2010, pp. 4772–4775.

[10] S.R. Cloude, *Polarisation: applications in remote sensing*, Oxford University Press, November 2009.

[11] S. Hensley *et Al.*, "The UAVSAR Instrument: Description and First Results," in *Radar Conference, 2008. RADAR '08. IEEE*, May 2008, pp. 1–6.

[12] Marc Simard, Scott Hensley, Marco Lavalle, Ralph Dubayah, Naiara Pinto, and Michelle Hofton, "An empirical assessment of temporal decorrelation using the uninhabited aerial vehicle synthetic aperture radar over forested landscapes," *Remote Sensing*, vol. 4, no. 4, pp. 975–986, 2012.